Finite Element Analysis of the Injury Potential of Shock-Induced Compressive Waves on Human Bone

A. M. Bailey[1], J. J. Christopher[1], S. Boruah,[1] M. Shafieian[1], D. S. Cronin[2], and R. S. Salzar[1]
[1]University of Virginia; [2]University of Waterloo

ABSTRACT

Recent military conflicts have provided evidence of a new mode of lower extremity injury as a result of under-vehicle blasts. Extreme vehicle design elements have decreased the frequency of hull breech into the occupant compartment, yet catastrophic injuries to the lower extremities continue to occur. Previous studies of shock wave-induced injuries, such as blast lung, have highlighted acoustic impedance mismatch as a potential injury mechanism, and in the under-vehicle blast scenario, a similar situation appears to exist. In under-vehicle blast, the lower extremities, with higher acoustic impedance, are loaded by a high speed compression wave (caused by the shock wave from a blast) through the low impedance vehicle armor. This mechanism loads the lower extremities faster than its respective speed of sound. Numerical analysis of this steel plate/lower extremity interaction reveals the potential for the accumulation of stresses in the high-impedance bone, which has potential to induce injuries separate from the more traditional inertia-based injuries. To prove the concept of acoustic impedance mismatch as an injury mechanism for this scenario, a series of finite element simulations were was developed examining the injury potential of a high speed compression wave traveling from a low impedance material into a higher impedance bone material. By varying both the amount of energy input and the amount of impedance mismatch between the armor material and the bone, the potential for significant energy accumulation is shown. Additional analysis of this phenomenon also reveals the importance of capturing the strain-rate dependent material properties of bone. The results of this study provide a foundation for understanding the nature of a unique class of underbody blast injuries as well as insight into potential lower extremity injury mitigation strategies.

INTRODUCTION

Efforts to improve the design of armored military vehicles by decreasing the amount of floor intrusion from under-vehicle blasts have revealed the existence of a formerly uninvestigated injury mechanism. While previous lower extremity injuries were attributed to the inertia-based loading associated with breaching of the occupant compartment or severe deflection of the floor plate, the more recent injuries cannot be explained in the same manner (Nelson, 2008). Relatively small deflections in the vehicle floor panels suggest another injury mechanism exists.

Attempts to reproduce these underbody blast injuries have focused on inertial loading of the lower extremity and have neglected to consider alternative injury mechanisms such as impedance mismatch or the destruction that could be caused by a high speed compression wave traveling through bone. Considering the medium through which the blast energy is delivered to the foot could provide insight into the reason for seeing injury at very small floor plate deflections.

Quenneville, et al. concluded that "factors in addition to force" such as impulse and energy have potential for contributing to tibia injury criteria under impulse loading (Quenneville, 2011). Using shorter duration impulses than previous experiments such as Yoganandan et al. (1996), the Quenneville et al. experiment resulted in lower peak forces prior to injury. While such results may be artifacts of the lack of skin and other soft tissues between the bone and steel plate or other differences in the experimental set-up, these results could also be evidence of a separate injury mechanism which causes bone to fail in a different manner.

Landmine explosion injuries are classified into four categories based on the aspect of the explosion that causes the injury. These types include primary (injuries caused by the shockwave), secondary (injuries caused by fragments and other projectiles), tertiary (injuries due to the acceleration of the vehicle or floor pan deformation), and quaternary (injuries due to increased temperature) (Ramasamy, 2011). While most underbody blast injuries are classified as tertiary (Ramasamy, 2011), some injuries from underbody blast are characteristically different than those deemed to be a result of inertial loading. Figure 1 provides an example of a fracture produced from high rate inertial loading and one produced by under-vehicle blast. Notice the more comminuted state of the under-vehicle blast fracture compared to the fracture produced by pure inertial loading.

Figure 1: Typical inertia-based distal tibia fracture (left) (Funk, 2001) vs. an under-vehicle blast mid-tibia fracture (right) (Ramasamy, 2011)

The goal of this study was to separate out the inertial loading and concentrate on the effect of shock wave propagation through the vehicle floor and into the lower extremities. Arepally, et al. divided the injury mechanisms into three categories: elastic, viscous, and inertial (Arepally, 2008). Of these categories, the elastic injury mechanism was of most interest to the current study due to its focus on the compression and tension of a body rather than the inertial loads caused by accelerations. While the inertial loading is still an important factor, this

experiment focused on the influence of the high speed compression wave on injury, separate from the global accelerations the body experiences.

When considering the possibility of acoustic impedance as a potential contributor to this mechanism of injury, it is important to understand the properties of the materials involved. The floor panels in military vehicles are made of metals such as steel, which have a large speed of sound, approximately 5800 m/s. According to various research articles, the speed of sound in bone (specifically the tibia) is between 3000 and 4000 m/s (Wiess, 2000; Falk, 2007; Miyatake, 2002). When an object or shock wave hits the outer surface of the vehicle floor pan, a high speed compression wave, traveling at the speed of sound of the material through which it is moving, will form and propagate through the material. In this case, the wave is traveling at around 5800 m/s. The wave will travel through the steel and then reach a material on its opposite surface, the occupant's lower extremity. At this interface, part of the wave will be transmitted through the boot/ankle and into the skeleton, and part will be reflected back into the steel. Despite the fact that part of the wave will be reflected, even a small fraction of the shock wave's energy transmitted has enough energy to produce injuries in the bone.

The objective of this research was to demonstrate the influence acoustic impedance has on failure in bone. To prove this concept, a series of finite element simulations were developed examining the injury potential of a high speed compression wave traveling from a low impedance material into a higher impedance bone material. By varying both the amount of energy input and the amount of impedance mismatch between the armor material and the bone, the potential for significant energy accumulation was demonstrated in the finite element simulations based on the experimental setup. Additional analysis of this phenomenon also revealed the importance of capturing the strain-rate dependent material properties of bone. The results of this study provide a foundation for understanding the nature of some under-vehicle blast injuries as well as insight into potential lower extremity injury mitigation strategies.

METHODS

The objective of this study was to demonstrate that loading a material by sending a high speed compression wave through a material of a higher speed of sound into a material with a lower speed of sound will produce failures in the higher speed of sound material prior to the onset of inertial loading. A 3-D finite element model was created in LS-Dyna to demonstrate this concept. First, inertial loading was eliminated from the model using the concepts of Newton's cradle and the split Hopkinson bar. The model consisted of an impactor, a transmitter bar placed on either side of the specimen material, and a deflector. Each of the parts was modeled as a cylindrical bar with a diameter of 19 mm. The transmitters, specimen, and deflector were 603, 241, and 60 mm in length. Additionally, to prevent errors associated with artificial contact stiffening, the surface nodes of the specimen in contact with the transmitter bars were made common. The impactor was placed 5mm from the end of the first transmitter bar and the deflector was placed in direct contact with the end of the second transmitter bar (see Figure 2).

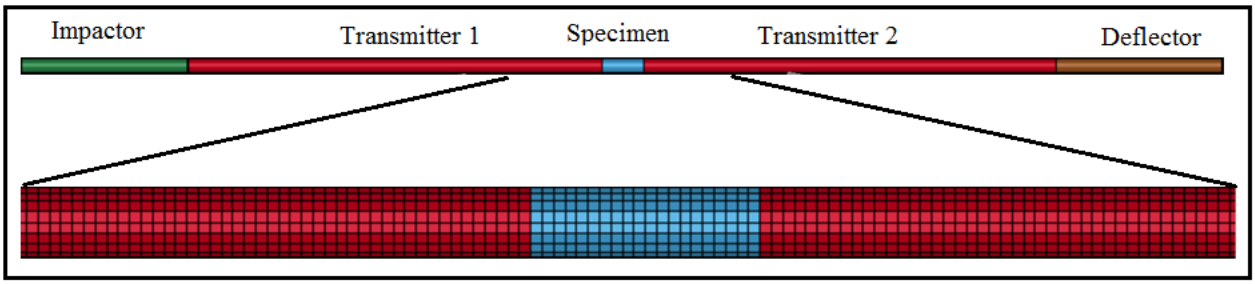

Figure 2: FE model showing common nodes between transmitters and specimen

For purposes of ensuring that the mass was balanced on either side of the specimen, the transmitters, impactor, and deflector were assigned the same material properties. The nodes of the impactor were given an initial velocity and allowed to impact the first transmitter bar; this generated a high speed compression wave that carried energy through the transmitter and into the specimen. After traveling through the specimen, the wave entered the second transmitter, and eventually the deflector. The deflector, because of symmetry in the design, then obtained a velocity, separating it from the second transmitter, and allowing the remaining parts to stay stationary and free of inertial loading as occurs in the Newton's cradle.

Several simulations were run using this finite element model in order to observe trends associated with the relationship between the material properties of the transmitter bars and the specimen. Initially, the impactor, transmitters, and deflector were assigned the properties of linear-elastic 2024 aluminum, and the specimen was given rate-dependent bone properties, outlined in this study. Two additional sets of simulations were run in which the material properties for the impactor, deflector, and transmitters were changed in order to modify the acoustic properties without changing the mass of these parts. To accomplish this, only the Young's modulus was altered, while the density remained equal to that of 2024 aluminum since the speed of sound for these models is calculated using the equation $c = \sqrt{E/\rho}$, where c is the speed of sound in the material, E is Young's modulus, and ρ is the density. The properties of all materials used are listed in Table 1.

Table 1: Material properties for finite element models

Material Name	Young's Modulus (GPa)	Density (kg/m^3)	Speed of Sound (m/s)
Aluminum 2024	73	2.78	5124
Modified Material 1 (MM1)	18.765	2.78	2598
Modified Material 2 (MM2)	40	2.78	3793
Rate Dependent Bone	13.5	2.00	2598

While bone is often modeled as an elastic material, studies such as the one done by McElhaney (McElhaney, 1966) on human femur cortical bone show that bone properties exhibit a strain-rate dependence. Cutting edge finite element biomechanical material models use a strain rate dependent plasticity model (*MAT_019 in LS Dyna) based on material testing results for

femur cortical bone (Untaroiu, 1997). For this study's finite element simulations, this material model was used for the bone material in which the tangent modulus is considered to be 5 percent of the Young's modulus and independent of strain rate (Bayraktar, 2004; Krone, 2006). The failure criterion for the material model was set to a plastic strain of 0.0088. A graph of the strain rate versus yield stress curve used for the bone material model is shown in Figure 3.

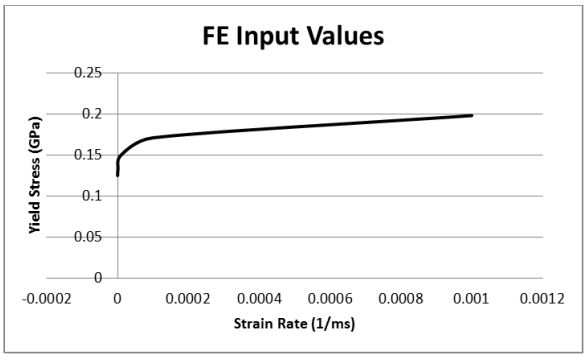

Figure 3: Yield stress for rate-dependent bone material model

For each of the three sets of material properties, a series of simulations were run with different initial velocities assigned to the impactor. Impactor velocities were 5, 15, 30, 40, and 50 m/s. For each, the longitudinal compressive strain wave was tracked through the bone specimen. Peak strain and internal energy were then plotted as a function of the distance along the bone specimen. This was important for determining the relationship between speed of sound and location of injury.

RESULTS

From the finite element simulations, strain data was recorded for elements along the length of specimen as well as at selected points within the transmitters. First, the strain time history was plotted for each of the elements in the bone specimen. The peak strain corresponding to the initial arrival of the compression wave at each element was then recorded for specific elements along the length of the bone specimen. This data is shown in Figure 4. Note that the strain peaks are consistent with the internal energy plots.

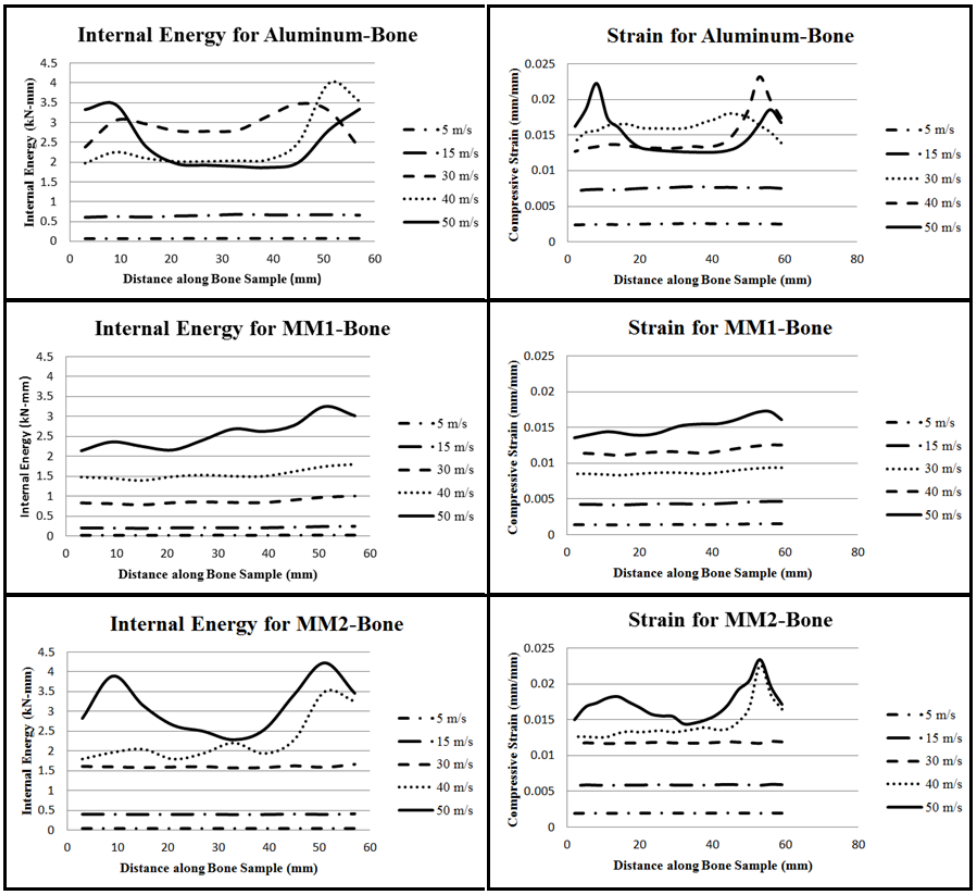

Figure 4: Strain and internal energy plots showing changes along length of specimen

For the case where the acoustic properties of the transmitters are equal to those of bone (material MM1), the strain varies almost linearly along the length of the bone with a very gradual slope. As the speed of sound in the transmitter was increased as for MM2 and then Aluminum, the strain developed peaks along the length of the bone. These peaks provide evidence that the speed of sound in the transmitters affects the amount of strain the bone material experiences.

It is also important to note that these strain peaks do not form for lower impactor velocities, which correspond to lower input energies; thus, a certain amount of energy is required to produce these strain elevations in the material. Additional simulations were run in order to determine the impactor velocity required to generate these drastic strain peaks. This velocity was determined to be around 35 m/s for the aluminum-bone interaction case. Figure 5, in which the time history for various elements is plotted, illustrates the onset of these strain spikes. Figure 6 displays similar plots for the case where the transmitters have the same speed of sound as the bone. Note the lack of strain peaks in this case.

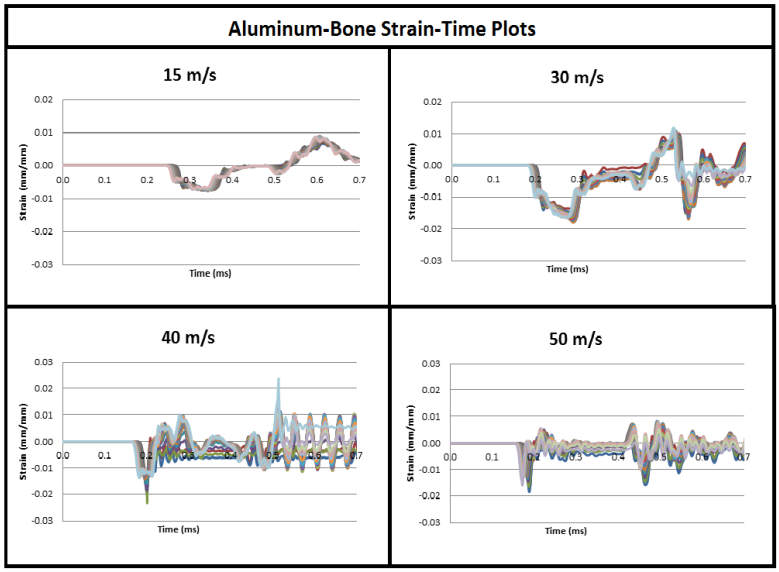

Figure 5: Strain plots for aluminum transmitter simulations
Note: Individual lines represent different elements along the length of the bone specimen

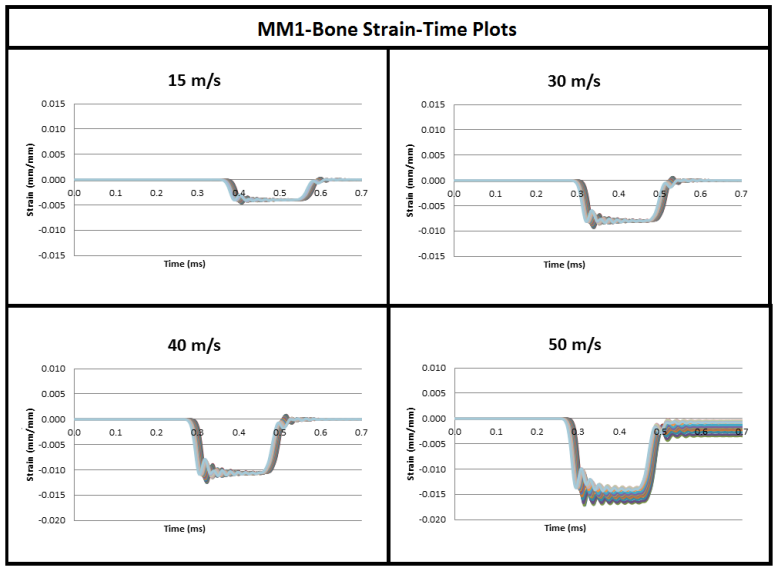

Figure 6: Strain plots for MM1 transmitter simulations
Note: Individual lines represent different elements along the length of the bone specimen

The material model used for bone allowed for observance of failure. All failures occurred upon the initial arrival of the high speed compressive wave and these locations are described in Table 2. The fact that fractures did not occur in the specimen where the bone and the transmitters had the same speed of sound (MM1) does not seem to be coincidental. Since the transmitter and the specimen had the same speed of sound, the high speed compressive wave created by the impact was able to move smoothly through the transmitter and then through the specimen. In the cases where an impedence mismatch existed, the strain (and stress) accumulated in the material due to the bone specimen's inability to move the wave through at the same rate it was being loaded by the transmitter. Since the wave speed was forced to decrease

because of its moving into a material with a higher impedance, the wave was forced to increase in amplitude to adjust, particularly in the cases where more energy was introduced into the system by increasing the impactor velocity.

Table 2: Element failure locations for finite element models

Model Description	Location of Failure
Aluminum-Bone at 40 m/s	54 mm from impact site
Aluminum-Bone at 50 m/s	12 and 54 mm from impact site
MM2-Bone at 40 m/s	54 mm from impact site
MM2-Bone at 50 m/s	54 mm from impact site

This is similar to what occurs in the proposed injury mechanism for the underbody blast scenario. A shock wave, carrying a large amount of energy, loads the underside of the vehicle, a steel plate. The plate allows the wave to travel through and into the lower extremities. Because of the mis-match in acoustic properties, a build-up of strain occurs in the lower extremity, and eventually reaches a point where the bone fractures catastrophically, producing injuries similar to that seen in Figure 1. Additionally, in cases where inertial loading is prominent, one would expect injury to occur near the impacted surface; however, certain underbody blast injuries appear to occur at mid-shaft of the tibia and more proximal (Figure 1). This would require peak strains or energies somewhere in the middle of the bone sample rather than at the contact surface. Figure 4 provides evidence of this phenomenon.

DISCUSSION

This finite element modeling effort has demonstrated the potential existence of a high-rate injury mechanism related to acoustic properties and the characteristics of a high speed compression wave. Anecdotal reports from theater suggest that comminuted injuries located at the mid-tibia can be explained by a combination of acoustic impedance mismatch between steel of the vehicle floor and the bone of the lower extremity, and the consequences of high-rate loading of rate-dependent biological materials. Fracture patterns produced in the FE model align with those of field injuries, and that cannot be explained by inertia-based loading. Additionally, eliminating the impedance mismatch in the model eliminated the strain and energy peaks which occur within the bone material, thus demonstrating the dependence of injury on the material through which a shock wave transmits energy.

CONCLUSIONS

While the key concepts of this injury mechanism are shown by the modeling approach taken, there are many additional factors to consider such as the tibial geometry and the inhomogeneity of bone. Furthermore, the effect of soft tissues in the foot/ankle and materials in the boot have the potential to damp the high speed compression wave before it enters the bone. Future modeling and experimental efforts will determine their contribution in damping the

transmission of the high speed compression wave. Future research will attempt to experimentally verify these finite element models. Moving forward, the results of this research may play a role in designing injury mitigation strategies for preventing under vehicle blast injuries, and should provide an explanation for some of the injuries reported from under vehicle blasts.

ACKNOWLEDGEMENTS

We would like to acknowledge the United States Army Aeromedical Research Lab (USAARL) and the United States Army Medical Research and Materiel Command (USAMRMC) for the funding of this project.

REFERENCES

AREPALLY, S., GORSICH, D., HOPE, K., GENTNER, S., DROTLEFF, K. (2008). Application of Mathematical Modeling in Potentially Survivable Blast Threats in Miliary Vehicles. Army RDECOM-TARDEC unclassified.

BAYRAKTAR, H.H., MORGAN, E.F., NIEBUR, G.L., MORRIS, G.E., WONG, E.K., KEAVENY, T.M. (2004). Comparison of the Elastic and Yeild Properties of Human Femoral Trabecular and Cortical Bone Tissue.

FALK, B., GALILI, Y., SIGEL, L., CONSTANTINI, N., ELIAKIM, A. (2007). A Cumulative Effect of Physical Training on Bone Strength in Males. International Journal of Sports Medicine, 28, 449-455.

FUNK, J.R., CRANDALL, J.R., TOURRET, L.J., MACMAHON, C.B., BASS, C.R., KHAEWPONG, N., EPPINGER, R.H. (2001). The Effect of Active Muscle Tension on the Axial Injury tolerance of the Human Foot/Ankle Complex. Proc. Enhanced Safety Vehicles Conference.

KRONE, R., SCHUSTER, P.S. (2006). An Investigation on the Importance of Material Anisotropy in Finite Element Modeling of the Human Femur. SAE International.

MCELHANEY, J. Dynamic Response of Bone and Muscle Tissue. (1966).

NELSON, T., CLARK, T., STEDJE-LARSEN, E.T., LEWIS, C.T., GRUNESKIN, J.M., ECHOLS, E.L., WALL, D.B., FELGER, E.A., BOHMAN, H.R. (2008). Close Proximity Blast Injry Patterns from Improvised Explosive Devices in Iraq: A Report of 18 Cases. Journal of Trauma, 65, 212-217.

QUENNEVILLE, C.E., MCLACHLIN, S.D., GREELEY, G.S., DUNNING, C.E. (2011). Injury Tolerance Criteria for Short-Duration Axial Impulse Loading of the Isolated Tibia. Journal of Trauma, 70(1).

RAMASAMY, A., HILL, A.M., HEPPER, A.E., BULL, A.M.J., CLASPER, J.C. (2011). Blast Mines: Physics, Injury Mechanisms, and Vehicle Protection. Philosophical Transactions of the Royal Society, 155(4).

RAMASAMY, A., MASOUROS, S.D., NEWELL, N., HILL, A.M., PROUD, W.G., BROWN, K.A., BULL, A.M., CLASPER, J.C. (2010). In-Vehicle Exremity Injuries from Improvised Explosive Devices: Current and Future Foci. Philospohical Transactions of the Royal Society, 366.

UNTAROIU, C., KERRIGAN, J., KAM, C., CRANDALL, J., AMAZAKI, K., FUKUYAMA, K, KAMIJI, K, YASUKI, T. (1997). Correlation of Strain and Loads Measured in the Long Bones with Observed Kinematics of the Lower Limb During Vechicle-Pedestrian Impacts. Stapp Car Crash Journal.

WEISS, M., BEN-SHLOMO, A.B., HAGAG, P., RAPOPORT, M. (2000). Reference Database for Bone Speed of Sound Measurement by a Novel Quantitative Multi-site Ultrasound Device. Osteoporosis International, 11, 688-696.

YOGANANDAN, N.F., PINTAR, F.A., BOYNTON, M. (1996). Dynamic Axial Tolerance of the Human Foot-Ankle Complex. SAE Paper.